

Thermo-Optical Property Degradation of Irradiated Spacecraft Surfaces

S. J. Leet,* L. B. Fogdall,[†] and M. C. Wilkinson[‡]

Boeing Defense and Space Group, Seattle, Washington 98124

The ionizing space radiation environment of energetic protons, electrons, solar ultraviolet radiation, and x rays is an established cause of thermal-control surface degradation. This work addresses the need for spacecraft thermal-control system designers to consider relevant degradation mechanisms when estimating end-of-life thermo-optical properties. A systematic approach is suggested as a first cut at estimating total solar absorptance and thermal emittance changes, based on available degradation data and spacecraft surface contamination levels. A particular example case of the degradation of space-facing surfaces at high altitudes was considered. For surfaces that do not view the sun and are at a sufficiently high altitude to be unaffected by atomic oxygen, charged-particle radiation bombardment and contamination are the two main degradation mechanisms. Measurements were made for the degradation of silver Teflon, Chemglaze A276 white paint, and fused-silica optical solar reflectors (OSRs) as a function of electron and proton fluence values. Data reveal dramatic darkening of Chemglaze white paint, substantial solar absorptance degradation in silver Teflon, and essentially no change in fused-silica OSRs. Recommendations are made for estimating the additional contribution of contamination degradation.

Introduction

THERMAL-PROPERTY degradation during on-orbit operations can be caused by charged-particle radiation, ultraviolet (uv) radiation, contamination, atomic oxygen, vacuum exposure, and temperature cycling. The charged-particle radiation damage for a given material is primarily a function of the spacecraft orbit, as is the level of atomic oxygen damage. The uv radiation damage is a function of spacecraft orbit and the orientation of the spacecraft surface relative to the sun. Degradation due to contamination is primarily due to surface deposition from spacecraft materials outgassing and from rocket exhaust contamination, and is therefore a function of spacecraft design. Contamination degradation can be more severe when the contaminant deposition occurs in the presence of uv radiation. The extent of degradation due to vacuum exposure and temperature cycling is related to the age of the spacecraft, as well as spacecraft operations.

The total degradation on a spacecraft surface is typically due to a complex synergism of all or some of these degradation mechanisms. Ideally, it would be of interest to perform accelerated ground tests that would simultaneously simulate the space and contamination environments for every type of external material used on the spacecraft. In this way, accurate end-of-life (EOL) thermo-optical properties could be used for EOL temperature predictions. Unfortunately, it is rarely practical or even possible to carry out such complex tests. Consequently, it is usually necessary to estimate the EOL properties from limited flight and/or ground test data and assessments of total spacecraft contamination levels.

In the following sections, a systematic approach is offered for evaluating EOL thermo-optical properties for spacecraft surfaces. A particular example case of the degradation of space-facing surfaces at high altitudes was considered. For surfaces that do not view the sun and are at a sufficiently high altitude to be unaffected by atomic oxygen, charged-particle radiation and contamination are the two main degradation mechanisms. Test data are provided for the degradation of silver Teflon[®], Chemglaze A276 white paint, and fused-silica optical solar reflectors (OSRs) as a function of charged-

particle radiation only. Recommendations are made for estimating the additional contribution of contamination degradation.

Analysis of EOL Thermo-Optical Properties

The approach taken to determine first-cut estimates of changes in solar absorptance ($\Delta\alpha_s$) and thermal emittance ($\Delta\epsilon$) values is to review pertinent data for the material(s) of interest. Careful evaluation of the available data relative to the application of interest is critically important. A series of questions should be considered when data are evaluated. For evaluation of flight degradation data, important questions are:

- 1) What is the orbit for which the flight data are acquired compared to the orbit of interest? What are the expected differences in electron and proton radiation fluences?
- 2) Does the surface face the sun? What was the uv radiation environment for the flight data relative to the expected uv radiation environment for the application of interest?
- 3) What was the contamination environment of the flight data? For example, is the surface for which degradation data are obtained in view of a main vehicle vent, or in view of another surface upon which vented materials can be reflected? What is the expected contamination environment for the application of interest? What are the maximum EOL contamination requirements for the application of interest versus the flight data? How are these requirements verified?
- 4) What are the differences in the atomic oxygen fluences between the flight data and the application of interest?
- 5) How long has the spacecraft for which flight data were acquired been in orbit relative to the lifetime of the application of interest? What was the duration of thermal vacuum testing for the spacecraft for which flight data were acquired relative to the application of interest? Is the total extent of temperature cycling similar?

For evaluation of ground degradation data, important questions are:

- 1) Is the total surface dose of electrons and protons expected to be the main driver in determining property degradation? Is the total depth dose an important consideration in evaluating the degradation? Or both? Do the properties of prime interest depend on surface phenomena (such as reflection or absorption of uv, which can occur in layers that are only micrometers thick), or are they dependent on effects occurring in a greater depth of material? Is it possible to assess the effect of performing accelerated short-term ground tests to simulate a substantially longer period of electron and/or proton penetration?
- 2) How important is the uv degradation? If the surface is constantly in the sun, then ground testing may not provide a conservative

Presented as Paper 93-2876 at the AIAA 28th Thermophysics Conference, Orlando, FL, July 6–9, 1993; received Nov. 9, 1993; revision received Jan. 24, 1995; accepted for publication Feb. 1, 1995. Copyright © 1995 by The Boeing Company. Published by the American Institute of Aeronautics and Astronautics, Inc., with permission.

*Space Systems Thermal Control/Contamination Engineer.

[†]Radiation Effects Scientist.

[‡]Space Environment Scientist.

enough database, since uv radiation cannot be accelerated much to simulate long life in space.

3) Was the effect of contamination deliberately or inadvertently included in the ground experiment? If contamination was not carefully controlled and/or measured, then significant degradation may be measured and reported as being a function of other parameters (such as uv radiation), when in fact the presence of contamination (or uv-enhanced contaminant deposition) may be causing the observed degradation.

4) Were atomic-oxygen effects satisfactorily simulated?

5) Was the experiment performed in vacuum at representative temperatures? Are there available data to assess the effect of performing short-term ground tests versus the degradation data that would be acquired at representative longer time periods?

After considering the above list of questions, degradation data are often discarded as irrelevant or as having limited value. For example, degradation data for leading-edge spacecraft surfaces in low Earth orbit (LEO) tend to be dominated by atomic oxygen effects, which may not be an important degradation mechanism for the higher-altitude orbits. Similarly, degradation data for spacecraft that suffer severe contamination (such as NAVSTAR) may be dominated by contamination effects over and above that which is typical of many spacecraft. Still other spacecraft, such as SCATHA, may be minimally contaminated. In this case, it may be necessary to add on an allowance to the observed $\Delta\alpha_s$ on SCATHA to estimate the total $\Delta\alpha_s$ for the application of interest.

Example of Estimating EOL Properties for Silver Teflon, White Chemglaze Paint, and Fused-Silica OSRs

Consider a spacecraft surface that is oriented away from the sun and will fly in a highly elliptical orbit (HEO), as on the Combined Radiation Release Effects Satellite (CRRES). For this situation, uv radiation effects are negligible. Erosion due to atomic oxygen was calculated for the CRRES orbit and found to be negligible as well. Charged-particle radiation damage and contamination are likely the two main degradation mechanisms for thermo-optical property degradation. The data acquired for silver Teflon, Chemglaze paint, and OSRs are listed in Table 1 and shown in Figs. 1 and 2.¹⁻⁷

In reviewing the list of important questions (see previous section), it is apparent that no data on charged-particle radiation damage are available for the CRRES orbit. The data generally are for, or are simulating, geosynchronous orbit and may therefore be inadequate, because the charged-particle environment for the CRRES orbit is different than the geosynchronous orbit. In general, the acquired data include the effects of uv radiation. Since the application of interest is for a non-sun-illuminated surface, the data may be overly conservative from this point of view. The degradation data also include the effects of contamination. However, it is not

readily apparent what portion of, for example, the degradation of silver Teflon (see Fig. 1) is a result of contamination or the synergistic effects of contamination, and what portion is due to other effects. The data representing spacecraft surfaces in LEO may include atomic-oxygen effects, which are not applicable in HEO.

Quartz mirrors are known to experience essentially no damage due to uv and charged particles; their increased solar absorptance is primarily due to contamination effects.¹ Therefore, the OSR degradation in Fig. 2 is primarily due to contamination effects. The data in Fig. 2 vary over a wide range, since each spacecraft is designed to vent differently, and each spacecraft vents different outgassing products onto its OSRs. The "recommended design curve for geosynchronous orbit" provides a 5-year degradation value of $\Delta\alpha_s = 0.13$ for OSRs. However, this value may underpredict the correct 5-year $\Delta\alpha_s$ value, if the spacecraft of interest is not vented properly, for example. For this reason, it is recommended to carry out a spacecraft contamination analysis based on materials outgassing and vehicle-level outgassing data and the spacecraft venting design, as described in the next section. Carrying out such an analysis should validate that spacecraft venting is acceptable in the vicinity of the OSRs.

Because of the limitations of the available degradation data, it was necessary to carry out charged-particle radiation tests on samples of Chemglaze A276 white paint, silver Teflon, and fused-silica OSRs. To reduce the complexity and cost of the testing, we decided to consider the effects of contamination separately, rather than to try to simulate experimentally the combined effects of contamination and charged-particle radiation. Fused-silica OSRs were included in the experiment to verify that the mirrors did not degrade in the presence of the charged-particle radiation. If degradation of the mirrors was

Table 1 Compilation of 5-year degradation data acquired for silver Teflon, Chemglaze A276 white paint, and fused-silica OSRs

Silver Teflon	Chemglaze A276 white paint	OSR
<i>Change in solar absorptance</i>		
See Fig. 1 (Ref. 1)	0.45 (Ref. 2)	See Fig. 2 (Ref. 1)
0.13 (Ref. 2)		0.17 (Ref. 3)
0.13 (15000 ESH, Ref. 4)		
0.08 (Ref. 5)		
0.11 (13000 ESH, Ref. 6)		
0.04 (10^{16} 40-keV p/cm ² , Ref. 7)		
0.03 (10^{16} 40-keV e/cm ² , Ref. 7)		
<i>Change in thermal emittance</i>		
0.00 (Ref. 2)	-0.02 (Ref. 2)	0.00 (Ref. 4)
0.03 (Ref. 4)	0.02 (Ref. 4)	
0.00 (Ref. 5)		

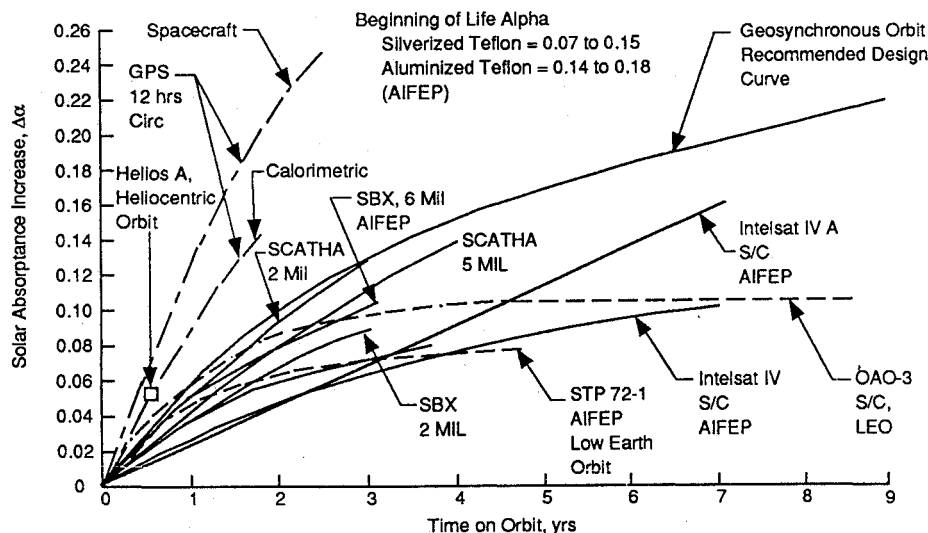


Fig. 1 Degradation of metalized Teflon (in geosynchronous orbit unless otherwise indicated). Reprinted with permission from Ref. 1.

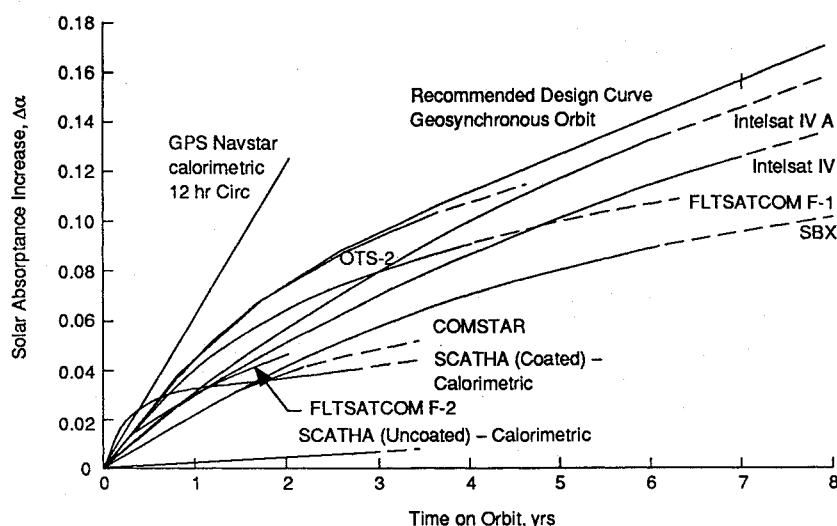


Fig. 2 Degradation of quartz mirrors in geosynchronous orbit (except GPS, which is not in GEO). Reprinted with permission from Ref. 1.

observed on the OSRs, then inadvertent contamination in the experiment would be suspected. In the following sections, the assessment of degradation due to contamination effects is described, and the charged-particle radiation testing is detailed.

Contamination Effects

The effects of contamination are among the most difficult degradation mechanisms to predict analytically or to simulate experimentally. On-orbit contaminant deposition is generally the result of outgassing from a variety of sources operating over a range of temperatures. Spacecraft materials outgassing and subsequent surface deposition are complicated functions of time, source temperature, receiver surface temperature, molecular conductance of the venting path, view factors, the molecular species of the outgassed material, and the presence of ultraviolet radiation, among other parameters. Thermo-optical property changes due to the presence of the contaminant film are a function of molecular species in the film, film thickness, morphology of the contamination, and the contaminant-substrate combination, among other parameters.

Typically, EOL contamination requirements are imposed on all contamination-sensitive surfaces of a spacecraft. These requirements are usually expressed in micrograms per square centimeter for molecular contamination and percent surface obscuration for particulate contamination. The contamination requirements are driven by spacecraft subsystem performance requirements. In the case of thermal-control-system requirements, a maximum allowable change in solar absorptance due to contamination is generally imposed. Spacecraft flight experience and laboratory experiments can be used to relate contamination levels to solar absorptance changes. A conservative correlation is that $1.0 \mu\text{g}/\text{cm}^2$ of molecular contamination deposition will increase the solar absorptance by 0.01. A conservative correlation for particulate contamination is that 1.0% surface obscuration will increase the solar absorptance by 0.01 (Ref. 8). The overall change in solar absorptance due to contamination may then be calculated as

$$(\Delta\alpha_s)_{\text{contamination}} = (\Delta\alpha_s)_{\text{molecular contam}} + (\Delta\alpha_s)_{\text{particulate contam}}$$

where

$$(\Delta\alpha_s)_{\text{molecular contam}}$$

$$= \frac{(0.01 \Delta\alpha_s)(\text{max allowed molecular contam})}{(1.0 \mu\text{g}/\text{cm}^2)}$$

$$(\Delta\alpha_s)_{\text{particulate contam}} = \frac{(0.01 \Delta\alpha_s)(\text{max allowed particulate contam})}{(1.0\%)}$$

It is usually assumed that the effect of contamination on thermal emittance is negligible, at least until a film thickness of $0.2 \mu\text{m}$ is

reached. This assumption is based on test data and the fact that most contaminants have optical properties in the infrared similar to those of the thermal-control surface.

Spacecraft contamination analyses are used to verify that EOL contamination requirements are met on contamination-sensitive spacecraft surfaces. The majority of particulate contamination on a spacecraft surface is typically due to ground processing operations and the launch and ascent environment. Ground analyses using facility fallout data in conjunction with a launch particulate redistribution model^{9,10} are often used to predict particulate contamination levels on spacecraft surfaces. Molecular contamination acquired on spacecraft surfaces is typically dominated by materials outgassing during on-orbit operations. Detailed analyses should consider the outgassing of all known nonmetallic materials used on the spacecraft. Usually an experimental outgassing database provides the basis for the analytic outgassing model. Internal molecular conductances should be calculated to determine the extent of outgassing from each spacecraft vent. Untaped Velcro and insulation openings around movable parts represent typical vent paths. View factors calculated between all spacecraft surfaces and vents, in addition to transient temperature predictions, are required input to a spacecraft contamination analysis. Ideally, the outgassing model should be correlated using quartz crystal microbalance (QCM) deposition data obtained during the spacecraft thermal vacuum testing. Finally, the effect of uv-radiation-enhanced deposition should be predicted quantitatively on the basis of available laboratory data correlating the contaminant deposition rate as a function of arrival rate (e.g., Ref. 11).

The outgassing deposition results generally vary from node to node on the spacecraft, and typically many nodes possess the same external material. Also, the outgassing deposition results are often updated whenever new outgassing data are implemented or a new material is added to the model (because of a spacecraft configuration change, for example). Therefore, it is usually impractical to use detailed analysis predictions to calculate the overall change in solar absorptance for each external material. If the results of the contamination analysis show that the EOL contamination requirements are met, then it is conservative to assume that the change in solar absorptance from contamination, including uv-radiation-enhanced deposition, is due to the maximum allowed EOL contamination levels.

An alternative approach is to estimate the change in solar absorptance due to contamination from laboratory data. A detailed survey of the location and abundance of all the nonmetallic materials composing the spacecraft (particularly internal materials), along with the spacecraft vents, will help identify the major contamination sources relative to a given external spacecraft surface. The laboratory experiment should consist of depositing outgassed material onto the material of interest and measuring the contamination level using a neighboring QCM. The change in thermo-optical properties as a

function of the contamination level can then be directly measured *in situ*.¹² If it is anticipated that the contaminant deposition will occur in the presence of radiation, then this effect should be included in the experiment as well.

Charged-Particle Radiation Effects on Chemglaze White Paint, Silver Teflon, and Fused-Silica OSRs

The interpretation of degradation data from spacecraft thermal-control surfaces is complicated by the variations in the charged-particle environments among orbits. For damage manifested as changes to thermo-optical properties, some thermal-control materials are altered mainly at their surfaces, and others are damaged in bulk. An example of the former is reduced reflectance of a metallic surface or an overcoating. Polymers such as Teflon and Kapton are examples of materials that can show significant damage to thermo-optical properties in bulk. Surface damage tends to come from low-energy charged particles, whereas higher-energy particles can penetrate to cause depth dose and damage along their penetrating tracks. Both surface and depth-dose effects should be considered when evaluating flight data as well as laboratory data.

The charged-particle fluxes incident on a spacecraft in geostationary earth orbit (GEO), SCATHA (near GEO), NAVSTAR (12-circular) and CRRES (HEO) orbits were evaluated from the National Space Sciences Data Center (NSSDC) particle flux maps.^{13,14} AP-8MIN and AE-8 for charged particles with energies greater than 100 keV. The effect of these charged-particle spectra on spacecraft materials depends on the atomic and molecular makeup of the material. Kapton polymer fairly approximates both Teflon and many paint coatings for the purpose of analyzing the interaction of particulate radiation. The yearly absorbed dose in Kapton was thus calculated as a function of depth and is shown in Fig. 3. For the GEO, near-GEO, and NAVSTAR orbits, the low-energy protons dominate the surface dose, but electrons dominate in producing dose beyond 1 mil (25 μm) of depth. For the CRRES (HEO) orbit, protons dominate in dose production out to several mils.

Figure 4 shows the total ionizing dose (TID) for the GEO, SCATHA, and CRRES orbits. The plot shows that for thicknesses between 0.25 and 5.0 mils (≈ 10 – $100 \mu\text{m}$), the average daily TID is 3 to 5 times higher in the CRRES orbit. Based on results pre-

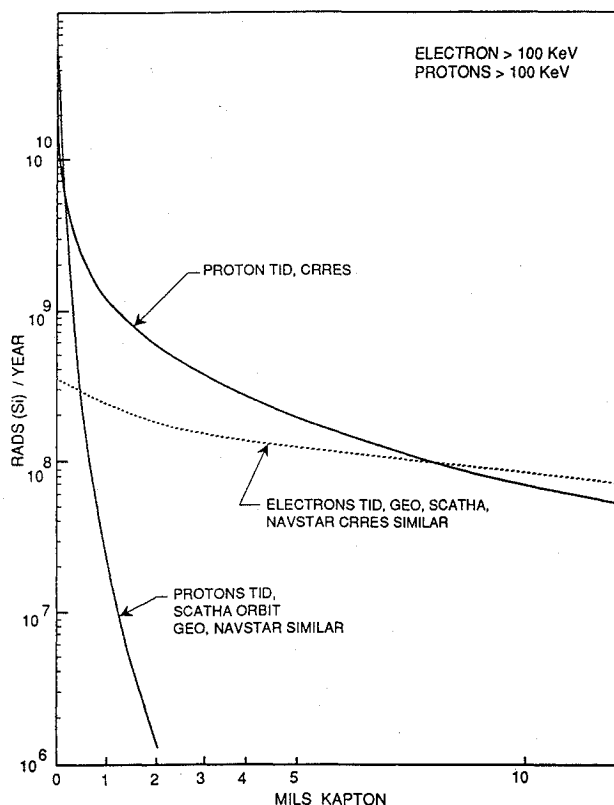


Fig. 3 Low-energy electron and proton ionizing dose.

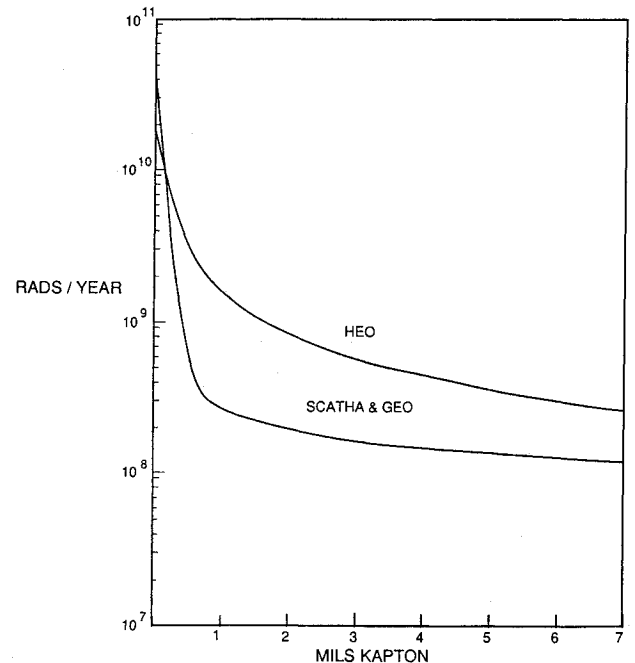


Fig. 4 Comparison of total ionizing dose.

sented in Figs. 3 and 4, it is reasonable to expect that the thermo-optical property degradation driven by surface damage is similar for the orbits considered. The actual surface dose is increased¹⁵ by the charged particles below 100 keV but these fluxes are not yet accurately modeled for the orbits of interest. In practice it is very difficult to simulate both surface and depth doses simultaneously, using laboratory sources of electrons and protons. In part this is because monoenergetic radiation sources are being used to represent energy spectra. In this exploratory work, the depth dose was not fully simulated; however, it is nevertheless recommended to do so whenever possible.

Experimental Setup

In this work, 40-keV protons and electrons were used to simulate the radiation dose near the material surfaces. The samples consisted of silver Teflon films, Chemglaze white-painted samples, and fused-silica optical solar reflectors. Specifically, the silver Teflon film was a metalized fluorocarbon film with 5 mils (125 μm) of Type A Teflon on vacuum-deposited silver on vacuum-deposited Inconel manufactured by Sheldahl. The white-painted samples were prepared in our laboratories by first spray-applying a 0.00025- to 0.0005-in. (0.00064- to 0.0013-cm) coat of thinned Lord Corporation Chemglaze Wash Primer on a copper substrate, then spraying a 0.002- to 0.003-in. (0.005- to 0.008-cm) topcoat of thinned Lord Corporation Chemglaze A276 White Paint. The optical solar reflector samples were manufactured by Sheldahl. These samples were a vapor-deposited silver coating on one surface of a fused silica substrate; the silver coating was overcoated with a vapor-deposited dielectric coating. After fabrication each sample was cleaned with ethyl alcohol and assembled onto an all-metal holder in a cleanroom. This array of test samples was then transferred double-bagged to the irradiation facility.

The samples were irradiated with electrons and protons simultaneously in the second-generation Combined Radiation Effects Test Chamber (CRETC II) at the Boeing Radiation Effects Laboratory. CRETC II is an ultrahigh-vacuum facility that has been used extensively for the study of spacecraft materials in simulated space-radiation environments. This facility captures the best features of earlier chambers, following a number of years of studying thermal-control coatings and other spacecraft materials under a variety of conditions for government and corporate customers. CRETC II features some advanced simulation capabilities along with providing a high-quality test environment, including a low-contamination vacuum. Vacuum conditions (typically 10^{-7} to 10^{-8} torr) are reached without resorting to organic or other potentially

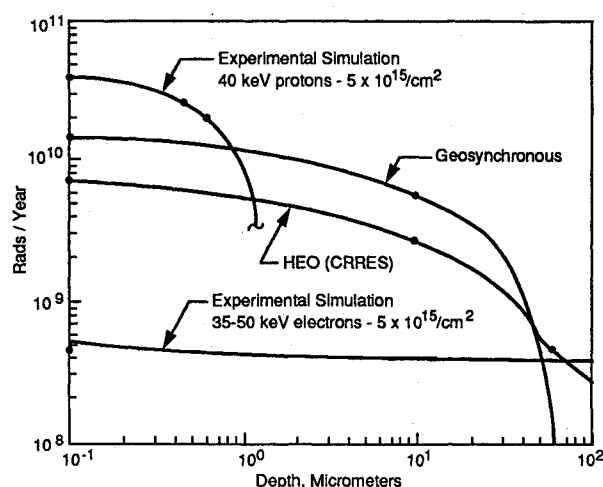


Fig. 5 Yearly dose near surface.

contaminating fluids. The evacuation sequence is dry-nitrogen-gas aspiration, cryosorption, large-surface LN_2 cold-trapping, long-term cryopumping, and ion pumping. Radiation exposure capabilities include the solar uv continuum, line-emission vacuum uv, and both electrons and protons. Electrons with energies between 20 and 70 keV and protons with energies between about 10 and 50 keV are commonly included in CRETC experiments, at near-real-time fluxes between 10^8 and 10^{10} particles/ $\text{cm}^2 \cdot \text{s}$. Beam uniformities of $\pm 10\%$ are common both spatially and temporally. The experimental work described here lasted more than a month, and simulated up to 16 years in orbit. The annual depth dose profiles expected for the OSRs and silver Teflon in the experimental simulation are shown in Fig. 5.

No solar or other ultraviolet radiation was included in the simulation, so as to study the effects of charged particles alone on these materials. To check repeatability of test results, multiple specimens of each material were irradiated concurrently.

The measurement of light reflection, absorption, and thermal emittance are fundamental for a complete evaluation of spacecraft thermal-control surfaces. Solar absorptance and thermal emittance data were obtained on silver Teflon films, Chemglaze white-painted samples, and fused-silica optical solar reflectors. All of these materials are at least somewhat specularly reflecting. Unirradiated Teflon and OSRs are highly specular, and Chemglaze A276 white paint has a gloss component in its visible reflectance. A high-precision spectral reflectance data system was used for the solar absorptance measurements in situ in CRETC, consisting of a dual-beam spectrophotometer and integrating sphere coupled to a personal-computer-based data-logging system. Wavelengths from 250 to 2500 nm were included. Both the specular and the diffuse components of reflection were detected, and the integrating sphere thus measured total hemispherical reflectance. A Gier-Dunkle DB-100 infrared reflectometer was used for the thermal emittance measurements.

The CRETC sample table uses internally circulating fluids to control temperatures of test samples. This control is uninterrupted between irradiation and measurement portions of test cycles, and was $20 \pm 5^\circ\text{C}$ during this program. The OSRs and the white paint samples on metal substrates were mounted with spring clips to make good thermal contact on the CRETC sample table. It was not desired by the test plan that the silver Teflon samples be rigidly bonded to metal substrates or chamber ground during irradiation. Instead they were wrapped around a section of aluminum cylinder during irradiation to increase thermal and electrical contact beyond that which a planar exposure configuration would have provided for unbonded polymer film. The protons' and electrons' angles of incidence were changed slightly by this wrapping, but only in nonmeasured areas.

One additional test was performed. Cobalt-60 gamma rays simulated the space radiation dose at greater depths, such as at the interface between 5-mil (125- μm) Teflon and its (second-surface) reflective silver layer. Silver Teflon was cobalt-irradiated at room temperature while bagged in polyethylene that had been purged with argon.

Test Results

Changes in the solar absorptance and thermal emittance of the materials as a function of radiation fluences are presented in Tables 2 and 3. The solar absorptance data were obtained in situ (i.e., without breaking vacuum), whereas the thermal emittance data were obtained in air. In the tabular data the first two digits are significant, and the third is retained and shown to indicate trends. The charged-particle fluence values listed in the left column of each table are abbreviated, and are to be interpreted as the number of particles of each sign, e.g., 4×10^{16} e/ cm^2 plus 4×10^{16} p/ cm^2 simultaneously over the same beam and sample area.

The in situ solar absorptance apparatus measures with accuracy ~ 0.02 or better, and with reproducibility better than ± 0.005 . Irradiation caused the solar absorptance of silver Teflon and the white paint to increase quickly to values much greater than the lower limits of measurability.

There was some concern from past experience¹⁶ that silver Teflon would build up electrostatic charge during irradiation and rather quickly become scattering or even opaque above its silver reflective layer. In this experiment, with electrons and protons irradiating the samples with approximately equal fluxes simultaneously, the Teflon remained specular (i.e., remained transparent through to its silver layer, and the overall specimen remained reflective) until the test was nearly half complete (2×10^{16} e/ cm^2 and 2×10^{16} p/ cm^2 fluences). Only then did the silver Teflon samples gradually dull as viewed through the chamber port, and slowly acquire a yellowish appearance (confirmed in the shape of the measured reflectance traces).

Reflectance measurement results showed that the Chemglaze white-painted samples quickly tanned, and by the end of the test these samples were nearly black. The test log notes that Chemglaze white paint was slightly tan at 1% of full dose, "caramel-brown" at 12% of full dose, and "more black than brown" at 50% of full dose. Our experience indicates that darkening of most white paint coatings is a function of total dose or fluence, rather than irradiation rate.⁷

The OSR rigid mirrors underwent no change that was visually apparent through the test chamber's viewport. More quantitatively, the measured changes in the spectral reflectance and solar absorptance of the OSR mirrors were found to be small—at or below the limit of experimental and instrumental accuracy. This is indicative of the low-contamination test environment and thus validates the use of the test data for understanding the effects of charged-particle radiation in the absence of contamination.

Test results in Table 2 have been summarized for all three materials in Fig. 6, where the change in solar absorptance versus the charged-particle fluence is plotted. (Each data point represents the

Table 2 Solar absorptance of Chemglaze A276 white paint, silver Teflon, and OSR mirrors in situ before and after irradiation

Fluence ^a	Absorptance		
	Chemglaze A276 white paint	Silver Teflon	OSR
Preirradiation	0.236	0.091	0.072
$>1 \times 10^{14}$	0.276	0.094	0.073
$>6 \times 10^{14}$	0.356	0.108	
2×10^{15}	0.532	0.110	0.074
$>5 \times 10^{15}$	0.671	0.133	0.071
2×10^{16}	0.777	0.192	0.080
4×10^{16}	0.793	0.282	0.087

^aElectrons and protons.

Table 3 Normal emittance of Chemglaze A276 white paint, silvered Teflon, and OSR mirrors in air at room temperature

Fluence	Emittance		
	Chemglaze A276 white paint	Silver Teflon	OSR
Preirradiation	0.883	0.791	0.800
4×10^{16} e and p	0.864	0.829	0.796
$\sim 10^6$ Gy γ		0.801	

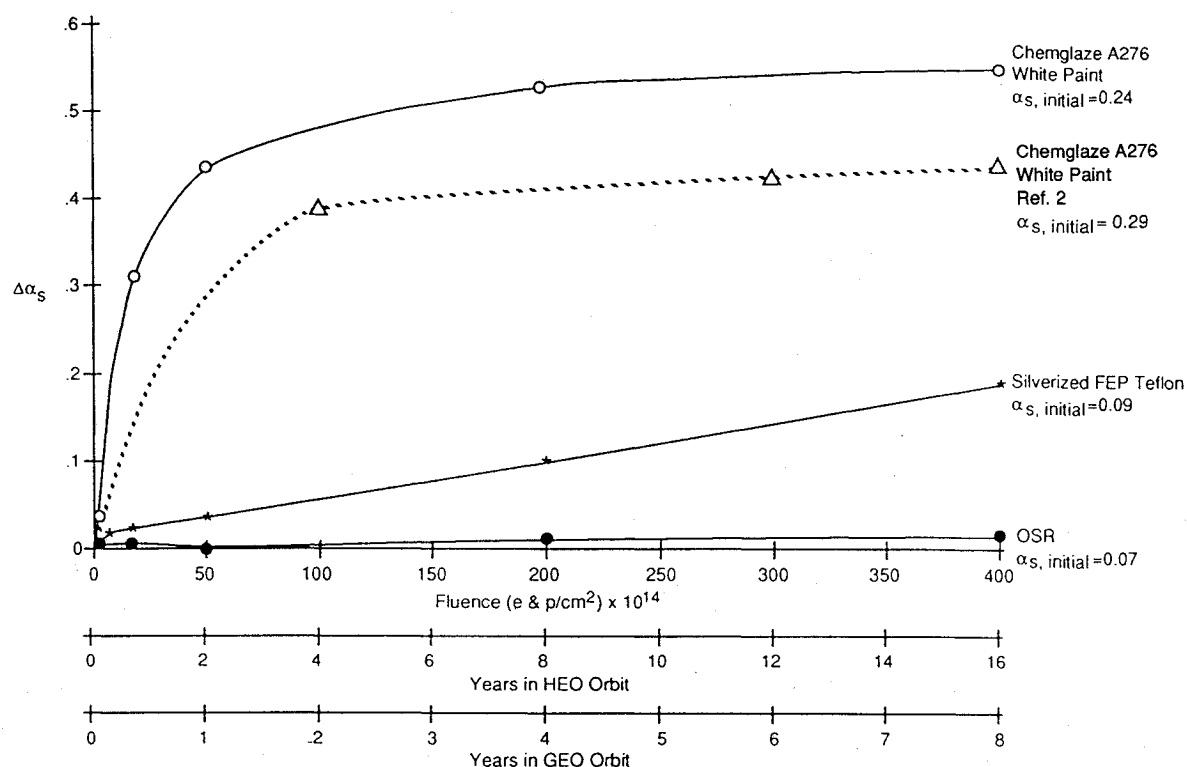


Fig. 6 Solar absorptance degradation results.

average of measurements from two or three samples.) The equivalent time in GEO and HEO orbits was calculated and is displayed along the horizontal axis in Fig. 6. Our test results from the irradiation of Chemglaze A276 white paint by protons and electrons have been compared with earlier data that were obtained after exposure to uv along with protons and electrons (Ref. 2 and dashed curve in Fig. 6). Figure 6 shows the degradation from protons and electrons alone always to be greater. Possible explanations include the fact that the paint's initial solar absorptance in the test with uv was 0.05 higher, and the earlier data was obtained in air. This second fact could by itself account for the difference, since it is widely established that there are in situ effects in spacecraft paint coatings. But the role of uv in partially "bleaching" or offsetting damage as recorded in situ is also possible. Similar bleaching or reduction of reflectance degradation measured in vacuum has been documented for other white paints.¹⁷ The minimal changes in OSR solar absorptance indicated in Fig. 6 shows that contamination had virtually no influence on these test results. The larger changes shown for silver Teflon and Chemglaze A276 white paint correspond to their darkening discussed previously.

Measurements of the thermal emittance of most of the test specimens were made in air using a directional-emittance measuring instrument. Because we expected only small changes in measured thermal emittance values after irradiation, and because the variability of thermal emittance among similar coupons should be even smaller, an approach of measuring all samples at one time was taken. This means that unirradiated, reserve specimens were used for "before" measurements, and irradiated samples were measured just moments before or afterward for comparison. Table 3 presents the data from these measurements in air. Multiple measurements of several specimens showed that reproducibility better than ± 0.005 could be obtained routinely. The instrument manufacturer claims ± 0.02 accuracy for directional emittance measurements. The changes in thermal emittance (unirradiated versus irradiated samples) reported in Table 3 for in-air measurements of proton + electron-irradiated Chemglaze A276 white paint and silver Teflon are believed to be real, since the differences are significantly greater than the reproducibility limits in one measuring session (minutes to hours).

The thermal emittance of silver Teflon exposed to Co^{60} gamma rays (10^6 Gy) was also measured in air. The results, included in Table 3, indicate no change in emittance as a result of the Co^{60}

irradiation. No embrittlement of the silver Teflon was observed, although its polyethylene enclosure was embrittled by the exposure.

Discussion

To compare the radiation effects expected from the space environment and the test environment produced by our space chamber, the depth dose profile in a typical thermal control material was calculated for GEO and HEO orbits. Then, the depth dose profile in the experimental simulation was calculated and compared with the expected space application (see Fig. 5). This approach assumes that the dominant damage mechanisms in the thermal-control surfaces are related to the ionizing dose in the material. Some limitations with this evaluation method are as follows.

First, defining the surface dose accurately in the space environment is difficult, since it requires knowledge of particle fluxes in the low keV region. These particle fluxes are quite variable with solar activity, and much less attention has been devoted to developing accurate flux maps in the low energy region than for energies greater than 100 keV. Recent data from CRRES have indicated that solar proton activity can have a profound effect on even the more stable proton fluxes, and the electron fluxes have long been known to vary widely with solar activity. The low-energy (less than 100 keV) electron and proton fluxes used to predict the surface dose in Fig. 5 were obtained by extrapolating the fluxes¹³⁻¹⁵ from AE-8 and AP-8MIN down to the low keV energy region. Therefore, the absolute values of the absorbed dose in the low energy region are not known accurately. However, we believe the comparison of the dose values reported here for the various orbits is meaningful.

Second, the inability of monoenergetic particle energies available in test facilities to duplicate the entire depth dose profile exactly means that damage effects at all depths were not being accurately produced in this testing. It would be necessary to develop an extremely sophisticated laboratory simulation scheme, involving a succession of both electron and proton irradiation energies and fluxes, applied to test materials over rather exacting exposure times, in order to duplicate more closely the doses deposited at all depths of material. Not all of the required energies (1 keV to 100 MeV and higher) would generally be available in one irradiation facility, though we are considering a partial expansion toward such capabilities. Even with advances in simulation, the differences in damage due to electrons and protons will need to be understood better. The

different damage mechanisms of which electrons and protons are capable include ionization and displacement of atoms in materials structures, as discussed in Ref. 18. A thorough study of material damage mechanisms is just one area in which further study could be pursued as a follow-up to this exploratory assessment.

Conclusions

A systematic approach has been suggested as a first way of estimating total solar absorptance and thermal emittance changes at EOL, based on representative degradation data and spacecraft surface contamination levels. For surfaces that do not view the sun and are at a sufficiently high altitude to be unaffected by atomic oxygen, charged-particle radiation bombardment and contamination are the two main degradation mechanisms. Test data are provided for the degradation of silver Teflon, Chemglaze A276 white paint, and fused-silica OSRs as a function of charged-particle radiation only. Specifically, the test results showed:

1) The reflectance of Chemglaze white paint is not stable during combined electron-proton irradiation. The degradation of reflectance begins at relatively low fluences of charged particles. Degradation could be characterized as catastrophic for charged-particle fluences greater than 10^{16} cm^{-2} .

2) The reflectance of silver Teflon loosely bonded to a grounded substrate changes with electron-proton exposure, but the degradation is not great until fluences $> 1 \times 10^{16}$ (charged particles)/ cm^2 are reached. Under the irradiation conditions used here, damage to silvered Teflon appeared to be related to the total dose and not due to high dose rates.

3) Fused-silica OSRs are stable after combined electron-proton exposure using the energies and fluences of this test. The small change in solar absorptance ($\Delta\alpha_s \sim 0.02$) is at the limit of the experimental accuracy. This small change in solar absorptance, measured after our simulation lasting about 800 h, indicates the maximum change that should be attributed to vacuum, temperature, and/or contamination effects in the experiment.

Since the test data do not include contamination effects simulating the spacecraft contamination environment, it is necessary to add on a contribution due to contamination. A first-cut approximation of the total change in solar absorptance at EOL is that it is the sum of the change due to irradiation by charged particles and the change due to contamination. Similarly, the total change in thermal emittance at EOL is the sum of the change due to charged-particle radiation and the change due to contamination. The values of $(\Delta\alpha_s)_{\text{contamination}}$ and $\Delta\epsilon_{\text{contamination}}$ can be determined using the approaches discussed in the Contamination Effects section. We emphasize that this approach makes the simplifying assumption that the effect of charged-particle radiation and contamination may validly be treated separately, when in fact synergistic effects will occur.

References

¹Gilmore, D. G., and Stuckey, W. K., "Thermal Control Finishes," *Satellite Thermal Control Handbook*, Aerospace Corp. Press, El Segundo, CA, 1994, pp. 4-10-4-11.

²Hardgrove, W. R., "Space Simulation Test for Thermal Control Materials," NASA CP 3096, Nov. 1990, pp. 267-285.

³Winkler, W., "Material Performance Under Combined Stresses in the Hard Space Environment of the Sunprobe Helios-A," *Acta Astronautica*, Vol. 10, No. 4, 1983, pp. 189-205.

⁴Donabedian, M., "Cooling Systems," *The Infrared Handbook*, rev. ed., Environmental Research Inst. of Michigan, 1985, pp. 15-78.

⁵Anon., "Mariner/Venus Mercury 1973 Spacecraft Program Final Report," JPL 953000, D208-37000-1, Jet Propulsion Lab., 1974, pp. 135-137.

⁶Fogdall, L. B., and Cannaday, S. S., "Effects of Space Radiation on Thin Polymers and Non-Metallics," *Heat Transfer and Thermal Control Systems*, edited by L. S. Fletcher, Vol. 60, Progress in Aeronautics and Astronautics, AIAA, New York, 1978, pp. 290-304.

⁷Fogdall, L. B., and Cannaday, S. S., "Proton and Electron Effects in Thermal Control Materials," NASA-CR-110715, May 1970.

⁸Hamberg, O., and Tomlinson, F. D., "Sensitivity of Thermal Surface Solar Absorptance to Particulate Contamination," SAMSO-TR-71-264, June 1971, pp. 1-8.

⁹Klavins, A., and Lee, A. L., "Spacecraft Particulate Contaminant Redistribution," SPIE Paper 777-27, May 1987, pp. 236-244.

¹⁰Bareiss, L. E., and Jarossy, F. J., "Impact of STS Ground/Launch Particle Contamination Environment on an Optical Sensor," *Spacecraft Contamination: Sources and Prevention*, edited by J. A. Roux and T. D. Mc Coy, Vol. 91, Progress in Aeronautics and Astronautics, AIAA, New York, 1984, pp. 73-95.

¹¹Stewart, T. B., Arnold, G. S., Hall, D. F., Marvin, D. C., Hwang, W. C., Owl, R. C. Y., and Marten, H. D., "Photochemical Spacecraft Self-Contamination: Laboratory Results and Systems Impacts," *Journal of Spacecraft and Rockets*, Vol. 26, No. 5, 1989, pp. 358-367.

¹²Shaw, C. G., Thornton, M. M., and Mullen, C. R., "Contamination Effects Test Facility," SPIE Vol. 777, *Optical System Contamination: Effects, Measurement, Control*, edited by A. P. M. Glassford, 1987, pp. 189-198.

¹³Vette, J. I., "The AE-8 Trapped Electron Model Environment for Solar Maximum and Solar Minimum," National Space Sciences Data Center, NSSDC-91-24, Nov. 1991.

¹⁴Sawyer, D., and Vette, J., "AE-8 Trapped Proton Environment for Solar Maximum and Solar Minimum," National Space Sciences Data Center, NSSDC-76-06, Dec. 1976.

¹⁵Sawyer, D., and Vette, J., "A Model of the Near Earth Plasma Environment," National Space Sciences Data Center, NSSDC-77-01, July 1977.

¹⁶Fogdall, L. B., and Cannaday, S. S., "Effects of High Energy Simulated Space Radiation on Polymeric Second-Surface Mirrors," NASA-CR-132725, Oct. 1975.

¹⁷Brown, R. R., Fogdall, L. B., and Cannaday, S. S., "Electron-Ultraviolet Radiation Effects on Thermal Control Coatings," *Thermal Design Principles of Spacecraft and Entry Bodies*, edited by J. T. Bevans, Vol. 21, Progress in Aeronautics and Astronautics, AIAA, New York, 1969, pp. 697-724.

¹⁸Fogdall, L. B., Cannaday, S. S., and Brown, R. R., "Electron Energy Dependence for In-Vacuum Degradation and Recovery in Thermal Control Surfaces," *Thermophysics: Applications to Thermal Design of Spacecraft*, edited by J. T. Bevans, Vol. 23, Progress in Aeronautics and Astronautics, AIAA, New York, 1970, pp. 219-248.

R. K. Clark
Associate Editor